Random Laser Action in Dye-Doped Polymer Media with Inhomogeneously Distributed Particles and Gain

applied sciences

MDPI

Article

Random Laser Action in Dye-Doped Polymer Media with Inhomogeneously Distributed Particles and Gain

Takashi Okamoto * and Masaki Mori

Department of Physics and Information Technology, Kyushu Institute of Technology, 680-4 Kawazu, Iizuka, Fukuoka 820-8502, Japan

* Correspondence: okamoto@ces.kyutech.ac.jp

Received: 23 July 2019; Accepted: 21 August 2019; Published: 24 August 2019

Abstract: The properties of random lasing are investigated for bubble-structure (BS) dye-doped polymer random media in which non-scattering and no-gain regions are distributed. Experimental results demonstrate that, for BS random media, spectral narrowing and a decrease in the number of spectral spikes occur for incoherent and coherent random lasing, respectively, resulting in an increase in the spectral peak intensity in both cases. These features were observed owing to the differences in the diffusion properties of the pumping and emitted lights.

Keywords: multiple scattering; random laser; bubble structure; polymer gain medium

1. Introduction

Random lasers (RLs) are light sources that can generate nearly coherent light with the use of scattering media with gain [1–6]. As the optical feedback for lasing is provided by the multiple scattering of light instead of well-defined cavities, the random spatial distribution of the refractive index in the media directly affects the random lasing action. Therefore, the modes of RLs are strongly related to the scattering properties of the laser medium [7,8]. Thus, several structures of disordered gain media for RLs have been reported. For a random gain medium of monodisperse particles, the effect of Mie resonances is observed in the emission spectrum, although the emitted light is multiply scattered among the particles [9–11]. A defect introduced in such a monodisperse medium concentrates and enhances light in the region around it [12]. The size and shape of the scattering particles affect the coherent and incoherent random lasing [13–15]. The experimental results demonstrate that the lasing threshold [13] and spectral linewidth [14] depend on the particle size, whereas the shape of the scatterers affects the peak intensity of the laser emission [14]. Considering the particle size distribution, polydispersed neodymium-doped powders exhibit a high lasing efficiency when compared with monodispersed powders [15]. The inhomogeneous distribution of scatterers also changes the efficiency of random lasing [16]; the lasing threshold of an RL with clustered particles decreases as the degree of particle aggregation is increased [17]. These studies have demonstrated that the emission properties of an RL can be improved by varying the topology of the disordered medium.

In a previous study [18], we investigated the emission from a bubble-structured (BS) RL with coherent feedback, in which spacer particles (SPs) with gain and irregular shapes, as well as scattering particles, were randomly distributed. These SPs created non-scattering regions; thus, the distribution of scatterers was inhomogeneous. The experimental results showed that the peak intensity of the emission spectrum was enhanced when SPs with average diameters in the wide range of 53–300 μm were dispersed. In the present study, we investigated incoherent random lasing from a BS RL, which, to the best of our knowledge, has not been studied before. In addition, we used different SPs and investigated their effect on the emission spectrum from both coherent and incoherent RLs. Non-scattering regions were controlled more systematically by using transparent spherical SPs with well-defined diameters.

We examined whether the spectral peak intensity of RL emission was enhanced when the SPs were small (diameter in the range of 30–100 μm) and had no gain.

2. Experimental

Figure 1 shows a schematic of the random structures used for the RLs. For comparison, a conventional medium (Figure 1a) in which scatterers were distributed homogeneously (homogeneous medium) was also examined. The random gain media were fabricated using transparent silica particles with the diameters of 30, 40, 60, and 100 μm as SPs. The scattering particles of TiO_2 with a diameter of 180 nm, together with SPs, were dispersed in a light-curable photopolymer (Adell K40) doped with Rhodamine 6G (R6G) laser dye with a density of 6.7×10^{-3} mol/L. The refractive indices of the TiO_2 particles were in the range of 2.7–2.8 (depending on the wavelength), whereas they were 1.5 for both the silica particles and the K40 polymer. The liquid polymer medium was then cured via illumination for 8 min using 405-nm violet laser light. Two samples were fabricated for each configuration of SPs and scattering particles.

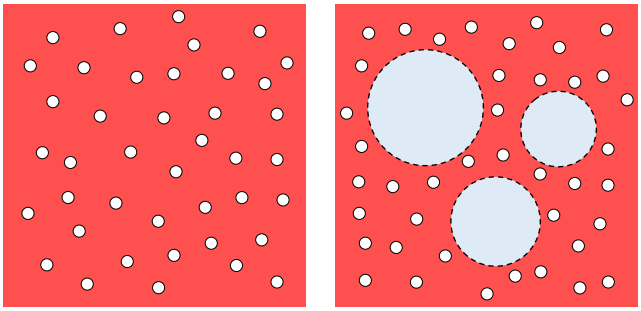

(**a**) (**b**)

Figure 1. (**a**) Homogeneous and (**b**) bubble-structure (BS) dye-doped scattering media. The white circles in (**a**,**b**) and the blue dashed circles in (**b**) represent scattering particles and spacer particles (SPs), respectively.

A schematic of the experimental setup is shown in Figure 2. The sample was pumped with a frequency-doubled Nd: YAG laser beam with a wavelength of 532 nm and a pulse duration of 10 ns. We used two different pump configurations: A pump with a circular excitation pattern and a pump with a stripe excitation pattern. The pump beam was focused onto the surface of the sample using a convex lens with a focal length of 50 mm for the circular excitation pattern, and a cylindrical lens with the same focal length for the stripe excitation pattern. For the circular excitation, the spot diameter was 62 μm and the excitation area was 3.0×10^3 μm^2, whereas for the stripe excitation, the stripe length was 2.7 mm and the excitation area was 0.57 mm^2. The light emitted from the sample was detected using a spectrometer (Ocean Optics HR2000) through a collector lens and an optical fiber at an observation angle of ~45°. The focal lengths of the collector lens were 50 mm for the circular excitation and 60 mm for the stripe excitation. A notch filter located in front of the fiber was used to remove the pump light. The emission spectrum was measured with a spectral resolution of 0.2 nm. For each sample configuration, 200 spectral data sets were obtained by varying the position of the pump spot. We fabricated and measured the samples with 5%, 10%, and 15% volume filling fractions of the scattering particles (ϕ_{sc}). The volume-filling fractions of the SPs (ϕ_{sp}) were 0%, 5%, 10%, and 15%. The SPs of each size occupied the same volume (for example, 2.5% for samples with 10% SPs).

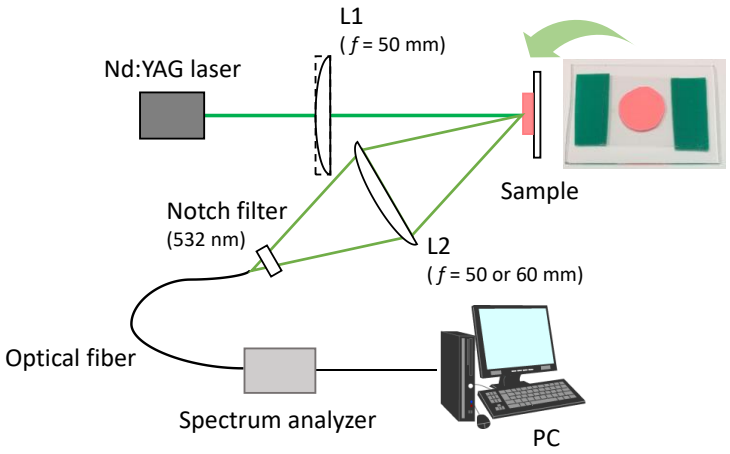

Figure 2. Schematic of the experimental setup for measuring random laser (RL) emission. L1 indicates a plano-convex lens or a plano-convex cylindrical lens, and L2 indicates a plano-convex lens.

3. Results

We observed two different spectral features of random lasing for different excitation patterns: Incoherent random lasing, which shows one broad spectral peak, and coherent random lasing, which exhibits several narrow spectral spikes.

3.1. Incoherent Random Lasing

We first examined the emission properties of BS RLs pumped with the circular excitation pattern. Figure 3 shows examples of single-shot emission spectra obtained from random gain media, with SPs (Figure 3b–d) and without them (Figure 3a). In addition, we measured the emission spectrum from samples with SPs and without scattering particles. An ordinary fluorescence spectrum was obtained, which was approximately the same as that measured without scatterers and SPs (K40 polymer with R6G only). This indicates that the SPs themselves do not produce laser action. We observed that incoherent random lasing occurred in all samples. As discussed later, the spectral peak becomes higher and its width becomes narrower when an appropriate volume fraction of SPs is added to the RL media.

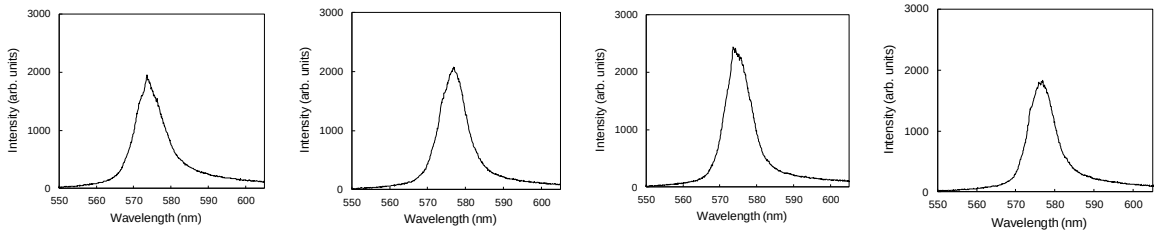

Figure 3. Emission spectra obtained with the circular excitation pattern for SP volume fractions of (**a**) 0%, (**b**) 5%, (**c**) 10%, and (**d**) 15%. The volume fraction of scattering particles is 10%. The pumping energy and energy density are 4 μJ and 1.3 mJ/mm^2, respectively.

The dependence of the spectral peak intensity on the pump energy is shown in Figure 4a. The slope efficiency of the BS medium is higher than that of the ordinary homogeneous medium. However, the lasing thresholds of the BS and homogeneous media are not noticeable. The lasing threshold can be identified in Figure 4b, where the spectral width is plotted as a function of the pump energy. The lasing thresholds for the BS and homogeneous media were in the range of 1.0–1.3 mJ/mm^2. For all pump energies, the spectral width is narrower for the BS medium than for the homogeneous medium.

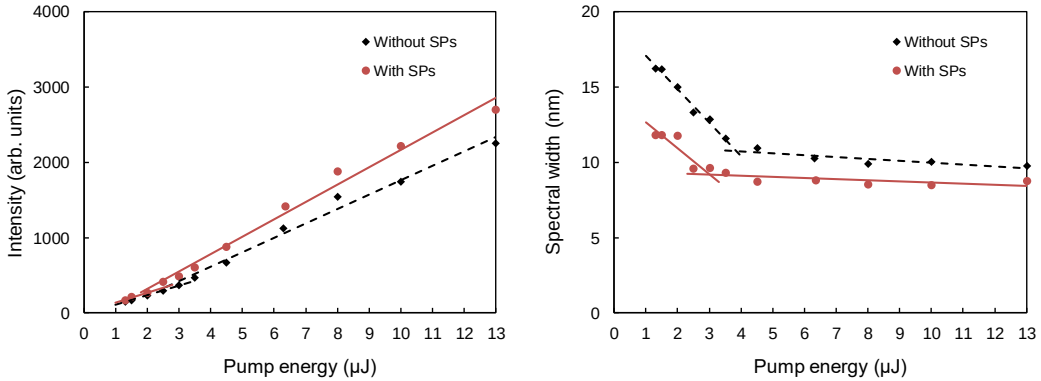

Figure 4. (**a**) Peak intensity of the emission spectra versus pump energy. (**b**) Full width at half maximum of emission spectra versus pump energy. The black rhombuses and red circles represent the homogeneous and BS media, respectively. The volume fraction of scattering particles is 10%, and the volume fraction of SPs in the BS medium is 10%.

There are two possible reasons for the increase in the intensity and for the spectral narrowing: (a) the difference in scatterer distributions and (b) the difference in scattering strength. We measured the transport mean free path (TMFP), l^*, for all samples, which is the inversely proportional to the scattering strength, using enhanced backscattering experiments [19]. Figure 5a shows the average value of the spectral peak intensity as a function of the TMFP. A high spectral peak was obtained at the TMFP in the range of 6–8 μm. When ϕ_{sc} is 10% (circles), the peak intensity for the BS media is ~30% higher than that for the homogeneous medium, even if the scattering strength is approximately the same. This result indicates that the enhancement of the spectral peak intensity results from the structural difference in the random media, and not from the scattering strength. The peak intensity of the BS media is also high for the ϕ_{sc} value at 5% (squares); however, the TMFP for the BS media is shorter than that for the homogeneous media. The opposite tendency is observed when ϕ_{sc} is increased to 15% (triangles). Therefore, there is an optimal concentration of scattering particles for the SPs that contribute to the increase in intensity.

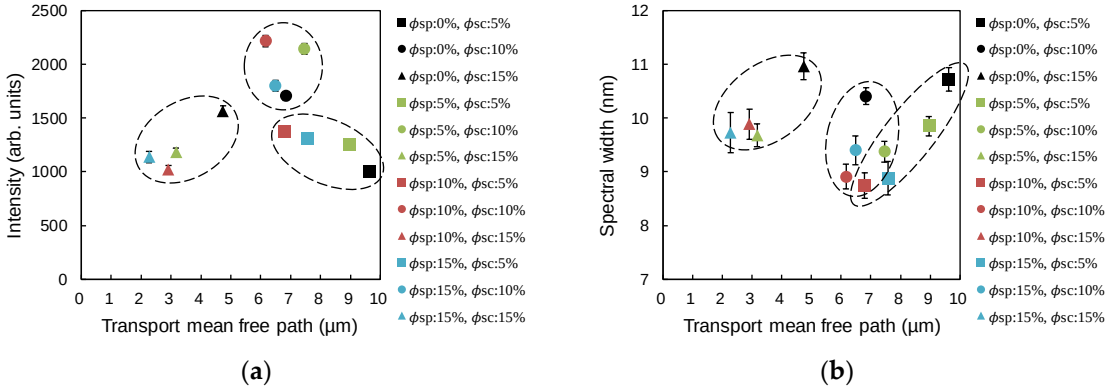

Figure 5. (**a**) Spectral peak intensity and (**b**) spectral width versus the transport mean free path (TMFP). Each dashed ellipse represents a group of the same volume fraction of scattering particles. The different colors represent the different volume fractions of SPs. The pumping energy and energy density are 4 μJ and 1.3 mJ/mm^2, respectively. The error bars represent the standard errors.

Figure 5b shows the relationship between the average spectral width and the TMFP. The spectral width is evidently independent of the TMFP. It was observed that all the BS media exhibit narrower spectral peaks when compared with the homogeneous media. As similar to the case of the peak intensity, the spectral width decreases by ~15% without significantly changing the TMFP when 10% SPs

are added to the 10% scatterer medium. The results shown in Figure 5 indicate that the inhomogeneity in the distribution of scatterers can improve the emission properties of incoherent RLs.

3.2. Coherent Random Lasing

Subsequently, we examined the emission properties of BS RLs pumped with the stripe excitation pattern. Figure 6 shows the single-shot emission spectra obtained from the BS media (Figure 6b–d) and from a homogeneous medium (Figure 6a). Several sharp spikes appear in the emission spectrum, indicating that coherent lasing can be achieved through stripe pumping.

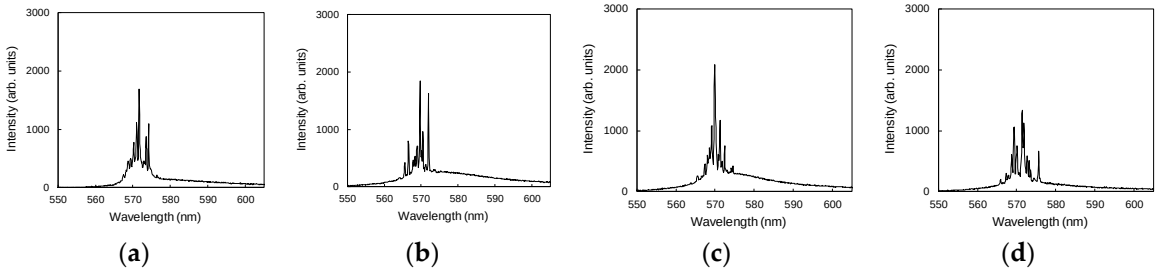

Figure 6. Emission spectra obtained with the stripe excitation pattern for SP volume fractions of (**a**) 0%, (**b**) 5%, (**c**) 10%, and (**d**) 15%. The volume fraction of scattering particles is 10%. The pumping energy and energy density are 13 μJ and 22.8 μJ/mm^2, respectively.

Figure 7a–c shows the average values of the maximum peak intensity, spike height, and number of spikes in the emission spectrum, respectively. The spike height is the intensity obtained after subtracting the incoherent pedestal component from the peak intensity. The maximum peak intensity shows the same tendency as the peak intensity for the incoherent random lasing shown in Figure 5a; the peak intensity and the maximum intensity become highest at 10% ϕ_{sc} (circles), when comparing the media with the same ϕ_{sp} but with different ϕ_{sc} values (data with the same color in Figures 5a and 7a). However, a large difference is observed for 15% ϕ_{sp} and 15% ϕ_{sc}: The maximum peak intensity shown in Figure 7a is very low. This is due to the negligible value of coherent lasing observable for this configuration. Figure 7b shows the same tendency as Figure 7a. This indicates that when the maximum intensity is high, the average height of all the spikes in the emission spectrum is high as well. It can be observed that the peak intensity for the BS medium with 10% ϕ_{sp} is ~20% higher than that for the homogeneous medium with 10% ϕ_{sc}, which is the same result as that obtained in [18]; however, the increase rate is lower in this case.

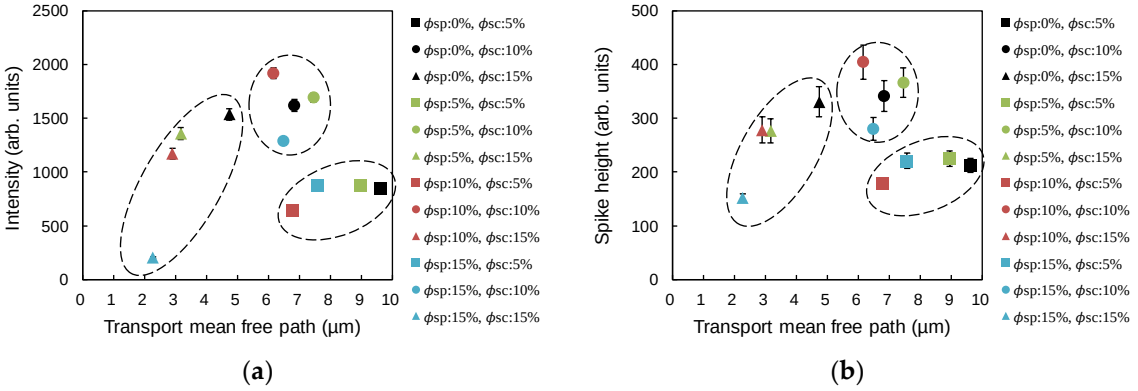

Figure 7. *Cont.*

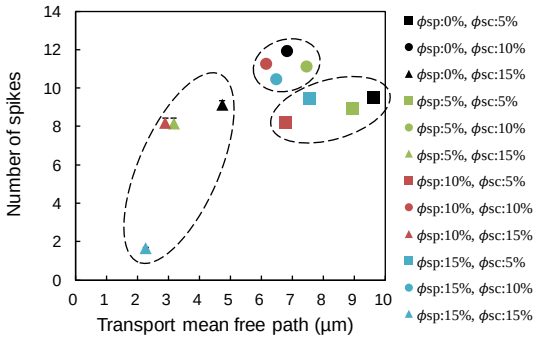

(**c**)

Figure 7. (**a**) Maximum peak intensity, (**b**) spike height, and (**c**) the number of spikes in the emission spectrum versus the TMFP. Each dashed ellipse represents a group of scattering particles having the same volume fraction. The different colors represent the different volume fractions of SPs. The pumping energy and the energy density are 13 μJ and 22.8 μJ/mm^2, respectively. The error bars represent the standard errors.

As shown in Figure 7c, the BS media have fewer spectral spikes than the homogeneous medium in each group of scattering particles having the same volume fraction. The comparison of the numbers of spikes for the media with TMFPs in the range of 6–8 μm suggests that the decrease in the number of spikes is mainly due to the structural difference of the random media.

To study the spectral spike height in more detail, we ranked the spikes by height and counted the number of spikes in each height range. The spike height distribution results for different ϕ_{sp} values are shown in Figure 8. As ϕ_{sp} increased from 0% to 10%, the number ratio of spikes with heights less than 200 decreased, whereas that of spikes with heights greater than 500 increased. Considering that the number of spikes reduced for the BS media, it was observed that the power spectral density concentrated on fewer wavelengths, resulting in a higher maximum peak intensity. When ϕ_{sp} was increased to 15%, the ratio of high spectral spikes decreased, and became less than that for the homogeneous medium.

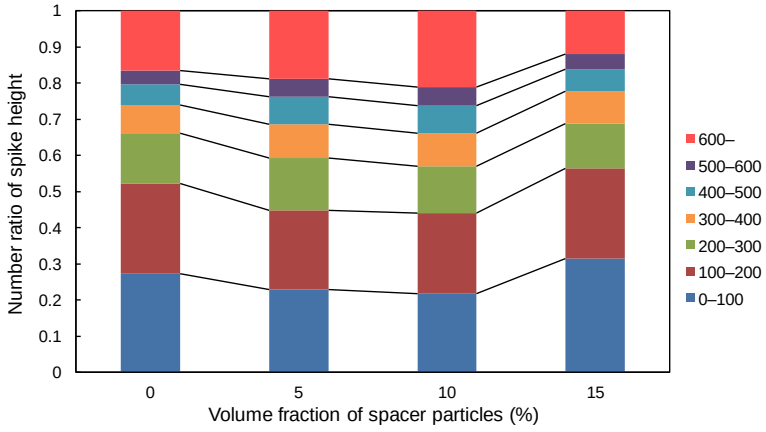

Figure 8. Ratio of the number of spectral spikes in different height ranges. The volume fraction of scattering particles is 10%. The pumping energy and energy density are 13 μJ and 22.8 μJ/mm^2, respectively.

4. Discussion

As discussed in Section 3, the BS RLs show spectral peaks higher than conventional RLs with dye and TiO_2 particles for both incoherent and coherent random lasing. In this section, the implications of the obtained results are discussed.

In our experiments, transparent particles without gain were used for the SPs. Thus, the volume of the medium, including the laser dye, is lower than that for the gain medium without SPs. Despite this decrease in the gain region, we observed a higher spectral peak and greater slope efficiency. This can be attributed to the difference in the distributions of pump lights. As discussed in Reference [18], the pump light spreads wider and deeper in the BS medium than in the homogeneous medium. In addition, the amount of pump light escaping from the subsurface region can decrease owing to the SPs near the surface; thus, the pump light is carried deeper into the medium. The pump region can also be increased by only reducing the volume fraction of scattering particles; however, this results in a weaker scattering strength and RL emission. Thus, more efficient pumping and lasing can be achieved by employing an inhomogeneous distribution of scattering particles in the BS media.

Subsequently, we observed that the spectral peak width decreased for the incoherent random lasing and that the number of spectral spikes decreased for the coherent random lasing. In a previous study [18], it was shown that the number of resonant wavelengths per mode decreased for the coherent lasing of BS RLs. Our new results for incoherent random lasing indicate that only light with wavelengths near the peak wavelength can remain. These results confirmed that the BS RLs exhibit stronger wavelength selectivity than the conventional RLs. One possible reason for this is the difference in the scattering free path and the path length distribution in the gain medium. Light exhibits normal diffusion in the homogeneous medium, whereas it undergoes a Lévy-like flight [20] in the BS medium. This anomalous diffusion of light can affect the selection of the emitted wavelengths. Further studies should be performed to understand this phenomenon.

Finally, we focus on the difference between the SPs used in this study and a previous study [18], where irregular-shaped and dye-doped particles with sizes in the range of 53–300 μm were used. In this study, we used transparent spherical particles with diameters in the range of 30–100 μm to determine whether the results obtained in the previous study were universal for BS gain media. According to the experimental results, the emission spectra exhibit the same characteristics, even if the SPs have no gain and have different shapes. The maximum peak intensity increased by ~40% for SPs with irregular-shaped and dye-doped particles with sizes in the range of 53–100 μm [18] (Figure 5). As shown in Figure 7a, the maximum peak intensity increased by ~20% for transparent spherical particles. The effect of the difference in the particle shape of SPs needs to be small, because neither scattering nor reflection or refraction occurs at the surface boundary of the SPs. Therefore, this difference is most likely due to the difference in the size distribution and the gain ability of the SPs.

5. Conclusions

We investigated random lasing action in dye-doped random gain media with a BS in which scatterers were inhomogeneously distributed. In a BS random medium, SPs in which no scatterer exists are introduced, such that the light is scattered differently when compared with the case of normal light diffusion. The SPs were transparent; thus, the light was amplified only in the other inhomogeneously distributed regions. The experimental results show that the spectral intensity becomes maximal for both incoherent and coherent random lasing when the appropriate volume fractions of scattering particles and SPs are dispersed in a random gain medium. We also observed a decrease in the spectral width and the number of spectral spikes. In a further study, our aim is to perform Monte Carlo simulations of photons to determine the behavior of light inside a BS random gain, and to understand the origin of these features exhibited by a BS RL. We hope that this study can support the design of random structures for high-performance RLs [21].

Author Contributions: Funding acquisition, T.O.; investigation, T.O. and M.M.; supervision, T.O.; writing—original draft, T.O.

Funding: This research was funded by the Japan Society for the Promotion of Science (JSPS) KAKENHI, under grant number 17K06388.

Acknowledgments: We thank Masanori Takabayashi for helpful discussions.

Conflicts of Interest: The authors declare no conflict of interest.

References

1. Wiersma, D.S. The physics and applications of random lasers. *Nat. Phys.* **2008**, *4*, 359–367. [CrossRef]
2. Cao, H. Review on latest developments in random lasers with coherent feedback. *J. Phys. A Math. Gen.* **2005**, *38*, 10497–10535. [CrossRef]
3. Noginov, M.A. *Solid-State Random Lasers*; Springer: New York, NY, USA, 2005.
4. Cao, H. Lasing in disordered media. In *Progress in Optics*; Wolf, E., Ed.; Elsevier: Amsterdam, The Netherlands, 2003; Volume 45.
5. Luan, F.; Gu, B.; Gomes, A.S.L.; Yong, K.T.; Wen, S.; Prasad, P.N. Lasing in nanocomposite random media. *Nano Today* **2015**, *10*, 168–192. [CrossRef]
6. Sznitko, L.; Mysliwiec, J.; Miniewicz, A. The role of polymers in random lasing. *J. Polym. Sci. B* **2015**, *53*, 951–974. [CrossRef]
7. Andreasen, J.; Asatryan, A.A.; Botten, L.C.; Byrne, M.A.; Cao, H.; Ge, L.; Labonté, L.; Sebbah, P.; Stone, A.D.; Türeci, H.E.; et al. Modes of random lasers. *Adv. Opt. Photonics* **2011**, *3*, 88–127. [CrossRef]
8. García-Revilla, S.; Fernández, J.; Barredo-Zuriarrain, M.; Carlos, L.D.; Pecoraro, E.; Iparraguirre, I.; Azkargorta, J.; Balda, R. Diffusive random laser modes under a spatiotemporal scope. *Opt. Express* **2015**, *23*, 1456–1469. [CrossRef] [PubMed]
9. Gottardo, S.; Sapienza, R.; García, P.D.; Blanco, A.; Wiersma, D.S.; López, C. Resonance-driven random lasing. *Nat. Photonics* **2008**, *2*, 429–432. [CrossRef]
10. Uppu, R.; Mujumdar, S. Persistent coherent random lasing using resonant scatterers. *Opt. Express* **2011**, *19*, 23523–23531. [CrossRef] [PubMed]
11. Gaio, M.; Peruzzo, M.; Sapienza, R. Tuning random lasing in photonic glasses. *Opt. Lett.* **2015**, *40*, 1611–1614. [CrossRef] [PubMed]
12. Fujiwara, H.; Niyuki, R.; Ishikawa, Y.; Koshizaki, N.; Tsuji, T.; Sasaki, K. Low-threshold and quasi-single-mode random laser within a submicrometer-sized ZnO spherical particle film. *Appl. Phys. Lett.* **2013**, *102*, 061110. [CrossRef]
13. Wu, X.H.; Yamilov, A.; Noh, H.; Cao, H.; Seelig, E.W.; Chang, R.P.H. Random lasing in closely packed resonant scatterers. *J. Opt. Soc. Am. B* **2004**, *21*, 159–167. [CrossRef]
14. Okamoto, T.; Adachi, S. Effect of particle size and shape on nonresonant random laser action of dye-doped polymer random media. *Opt. Rev.* **2010**, *17*, 300–304. [CrossRef]
15. Wetter, N.U.; Giehl, J.M.; Butzbach, F.; Anacleto, D.; Jiménez-Villar, E. Polydispersed powders (Nd^{3+}:YVO_3) for ultra efficient random lasers. *Part. Part. Syst. Charact.* **2018**, *35*, 1700335. [CrossRef]
16. Sciuti, L.F.; Gonçalves, T.S.; Tomazio, N.B.; de Camargo, A.S.S.; Mendonça, C.R.; De Boni, L. Random laser action in dye-doped xerogel with inhomogeneous TiO_2 nanoparticles distribution. *J. Mater. Sci. Mater. Electron.* **2019**. [CrossRef]
17. Leonetti, M.; Lopez, C. Random lasing in structures with multi-scale transport properties. *Appl. Phys. Lett.* **2012**, *101*, 251120. [CrossRef]
18. Okamoto, T.; Yoshitome, R. Random lasing in dye-doped polymer random media with a bubble structure. *J. Opt. Soc. Am. B* **2017**, *34*, 1497–1502. [CrossRef]
19. Akkermans, E.; Wolf, P.E.; Maynard, R. Coherent backscattering of light by disordered media: Analysis of the peak line shape. *Phys. Rev. Lett.* **1986**, *56*, 1471–1474. [CrossRef] [PubMed]
20. Barthelemy, P.; Bertolotti, J.; Wiersma, D.S. A Lévy flight for light. *Nature* **2008**, *453*, 495–498. [CrossRef] [PubMed]
21. Lee, M.; Callard, S.; Seassal, C.; Jeon, H. Taming of random lasers. *Nat. Photonics* **2019**, *13*, 445–448. [CrossRef]